

Supplementary Information

Gradient-multiscale-interconnected architectures enable waterborne superomniphobic surfaces to resist high-strength impact of solids and fluids

Fang Suo,^{ba} Boxu Chen,^a Zhenqiang Lin,^a Xin Yan,^a Yinglei Zhai,^b Jinyi Zhong^{ab} and Jingwen Liao^{*abc}

^a Interdisciplinary Plasma Engineering Centre, Guangzhou Institute of Advanced Technology, Guangzhou 511458, China

^b Department of Biomedical Engineering, School of Medical Devices, Shenyang Pharmaceutical University, Shenyang 110016, China

^c Shenzhen Institutes of Advanced Technology, Chinese Academy of Sciences, Shenzhen 518055, China

Experimental

Materials

If not otherwise specified, the chemicals of analytical grade are purchased from Aladdin Chem Co., and used without further treatment. The SiNPs (45 nm in diameter) are provided by Shanghai Yien Chemical Technology Co.. The HA (Solvesso 100, ExxonMobil Chemical) is supplied by Shanghai King Chemical Co.. All resin aqueous solutions are obtained from Shanghai Kaiyan Chemical Co..

Synthesis of poc-FPOSS–2OH

As reported in our previous works,¹⁻³ 0.2 mL H₂O, 2.55 g 1*H*,1*H*,2*H*,2*H*-perfluorooctyltriethoxysilane (FAS-13) and 200 mg NaOH is added in sequence in a typical 100-mL round-bottom flask filled with 20 mL THF, followed by magnetic stirring and refluxing at 70 °C for 5 h. Then, the round-bottom flask is kept at room temperature for 12 h. A sticky product is obtained after solvent removal in a rotary

evaporator at 55 °C and rinsing with 10 mL THF for 3 times at room temperature. The rinsing with THF as a purification procedure is necessary for eliminating side-products (mainly including oligomers of FAS). The high-purity sticky matter (the yield exceeds 85%), i.e., poc-FPOSS-2OH, is yellowish and stored with 35 mM in absolute ethanol (Fig. S1).

Preparation of FPOSS-SiNPs

In a typical 100-mL round-bottom flask filling with 50 ml absolute ethanol, 1.6 g SiNPs (with a size of ~45 nm in diameter) and 5 mL poc-FPOSS-2OH/ethanol (35 mM) is added and followed by magnetic stirring (1000 rpm) for 10 min and ultrasonication for 5 min. With a constant-pressure dropping funnel, 10 mL HCl (0.1 M) is added dropwise (a drop per 10 s) under magnetic stirring (500 rpm). The acid causes protonation of poc-FPOSS-2OH (poc-F13POSS-2OH₂⁺ as a result) and the SiNPs are wrapped by poc-F13POSS-2OH₂⁺ through 5 h incubation at room temperature. Finally, FPOSS-SiNPs (poc-FPOSS-wrapped SiNPs) are obtained after a 12 h-drying (Fig. S2).

Fabrication of SOSs

10 mLDMC with 0.5 mL poc-FPOSS-2OH/ethanol, 0.6 mL HA, 3.5 g FPOSS-SiNPs and 150 mL resin aqueous solution (with a solid content of 20%, waterborne air-drying polyurethane if not otherwise specified) are mixed in a 500-mL narrow-mouth bottle, followed by a fierce dispersion under 15000 rpm for 10 min in high shear dispersing emulsifier (Fluko FA25D, China). A white waterborne emulsion is formed as a result and stored in a sealed container. Using a sprayer without specific requirements, most substrates can be coated with this waterborne emulsion (300 μm in thickness). After air-drying for 8 h at room temperature, the waterborne emulsion is fully cured and a white GMI-SOS is born. When the “air-drying for 8 h at room temperature” process is replaced by immediate 150 °C for 5 min after spray-coating, the MI-SOS is produced. When the HA or FPOSS-SiNPs is removed to obtain waterborne emulsion, the GM-SOS or GI-SOS is separately fabricated.

Characterizations and measurements

Characterizations: The FE-SEM (ZEISS Gemini 500, Germany) is employed to probe

the morphology of specimens. The X-ray photoelectron spectroscopy (XPS) is used to ascertain the element distribution of SiNPs and FPOSS-SiNPs. The Zetasizer (Malvern Panalytical Advance Pro, Britain) is utilized to analyze particle size distribution of waterborne emulsion.

Contact angle measurement: The contact/roll-off angle measurements of specimens were performed using a surface contact angle analyzer (KSV Helsinki CAM200, Finland) with a 2 μL of liquid droplet at ambient temperature. The liquid droplets included liquids with various surface tension and kinematic viscosity (dimethyl silicon oil), and a series of non-Newtonian liquids. The non-Newtonian liquids covered milk, tomato sauce, soy sauce, egg white, goat blood, silicone oil, crude oil, sodium alginate (2 wt%) in water, chitosan (2 wt%) in acetic acid solution (1 wt%), PMMA (polymethyl methacrylate, 10 mg mL^{-1}) in DMF (dimethyl formamide), PMMA (10 mg mL^{-1}) in NMP (methyl pyrrolidone), PS (polystyrene, 10 mg mL^{-1}) in DMF, PS (10 mg mL^{-1}) in NMP, PVDF (polyvinylidene fluoride, 10 mg mL^{-1}) in DMF, PVDF (10 mg mL^{-1}) in NMP, PVDF-HFP (poly(vinylidene fluoride-co-hexafluoropropylene, 10 mg mL^{-1}) in DMF, PVDF-HFP (10 mg mL^{-1}) in NMP, PVP (polyvinyl pyrrolidone, 10 mg mL^{-1}) in DMF, PVP (10 mg mL^{-1}) in NMP.

Optical transmittance measurement: The optical transmittances of waterborne emulsion are measured using ultraviolet-visible (UV-Vis) spectrophotometer (HACH DR6000, USA) with a wavelength 560 nm. The cuvette is filled with 2 mL of waterborne emulsion, and the optical transmittances of both top and bottom sites are recorded at an interval of 10 min (Fig. S5A). For measurement at bottom site, the height of cuvette in fixator is adjusted to the highest point. For measurement at top site, because liquid level of emulsion in cuvette slowly drops down with water evaporation, the continuous height adjustment of cuvette in fixator is necessary to make visible light transmit through top site. Among the interval of 10 min, the cover of spectrophotometer is kept open, that is, the emulsion is in an open space. When a lip is introduced to seal the cuvette, the emulsion is in an enclosed space.

Droplet impact test: Dynamic bouncing process of dodecane droplet is investigated

with a high-speed camera (1000 frames per second, QianSheng NPX-GS6500UM, China) at ambient temperature. An 8 μL of dodecane droplet is released at a specific height and then impact the horizontal specimens. The release and impacting/bouncing processes of dodecane droplet is recorded by the high-speed camera.

Jet impact test: the water or ethanol jets are made through a car washer-used nozzle (its outlet has an inner diameter of 1.2 mm) connected with an air compressor. The high-pressure-air from air compressor force the normal-pressure water or ethanol to eject high-speed water or ethanol jets through the nozzle. The water or ethanol jets impact the horizontal specimens at a height (the distance between faucet or nozzle and specimens) of 20 cm (if not otherwise specified) for 5 times (20 s each time). The speeds of water or ethanol jets are calculated by cross-sectional area of cylinder jets and as-collected water or ethanol volume in a fixed time.

Taber abrasion test: Abrasion tests are performed following ASTM D3884 using a Taber abrasion tester (Shanghai Qingbo, China) under three loads of 250 g, 500 g and 1000 g. The SOSs on circular titanium plates with 108 mm in diameter, and a hole with 8 mm in diameter is drilled in the center of the specimens to fix it on the rotary platform of the Taber machine. According to the standard, the specimens running one rotation is counted as one abrasion cycle. The contact angles of SOSs are measured as a function of Taber abrasion cycles. Prior to contact angle measurements, the detached abrasive particles or any fragments on the specimens should be rinsed off.

Hammer impact test: These tests are conducted using a coating impact instrument (Shenzhen Haibin QCJ-0.5, China) equipped with a metal hammer of 1000 g in weight and 8 mm (punching head) in diameter. The SOSs on titanium plates with 80 mm \times 80 mm in size, are impacted by the metal hammer as a falling body released at various heights. The hammer impact need to continuously repeat 3 times to each specimen. The impact kinetic energy (E_k) of metal hammer is calculated by the release height (converting it to impact velocity v) and hammer weight (m), i.e., $E_k = 0.5mv^2$.

Evaporation experiment for Laplace pressure: A 5 μL water droplet is placed on a SOS

with GMI, GMs or MI, and its natural evaporation is allowed in air with humidity of $20 \pm 1\%$ at room temperature. In the whole evaporation process, the side-view profile of the droplet is recorded per 5 s by camera of surface contact angle analyzer. At last, the change of both contact angles and TPCL lengths of the water droplet with Laplace pressure ($P_l = 2\gamma/r$) is recognized via ImageJ software. The detailed calculation method of P_l can be found in Fig. S9 and Equation S3.

Mechanical characterization for force curve: The mechanical properties of the three types of SOSs in terms of force curves are evaluated by a Nano Indenter (KLA G200, USA). The Nano indenter have an expanded load capacity up to 10 N, and its indenter is equipped with a spherical diamond of 100 μm in diameter. Elasticity modulus mode is applied to measure the mechanical strengths. The indentation is carried out using a loading/unloading rate of 200 mN min^{-1} to reach a load of 0.5 and 4 N.

Ultrasonic resistance test: The SOSs are immersed into water and sonicate (power: 480 W) for scheduled times. Subsequently, the contact and roll-off angles of specimens are measured.

UV resistance test: The SOSs are exposed to ultraviolet (radiation wavelength: 365 nm, power density: 20 mW/cm^2) for various times. Subsequently, the contact and roll-off angles of specimens are measured.

Humidity resistance test: The relative humidity of 20 and 80% is set in a temperature & humidity test chamber (NOVTEC EST-1000-5, China), and the SOSs are placed for predetermined times at room temperature. Subsequently, the contact and roll-off angles of specimens are measured.

Hot/cold cycle resistance test: The SOSs are transferred into in temperature & humidity test chamber at room temperature and the temperature is raised up to 100 $^{\circ}\text{C}$ at a rate of 5 $^{\circ}\text{C/min}$ and keep 1 h. Then, the temperature is lowered down to -40 $^{\circ}\text{C}$ at a rate of -5 $^{\circ}\text{C/min}$ and keep 1 h. In this way, a hot/cold cycle is achieved. Through scheduled hot/cold cycles, the contact and roll-off angles of specimens are measured.

Acid/base resistance test: The SOSs are immersed in an aqueous solution with pH 1

(HCl) or 14 (NaOH) for various times at room temperature. Also, the SOSs are immersed in concentrated hydrochloric acid (36%~38%, strong acid) or concentrated ammonia solution (28~30%, strong base) for various times. Subsequently, the contact and roll-off angles of specimens are measured.

Organic solvent resistance test: The SOSs are immersed in petrol, toluene or butyl acetate for various times at room temperature. Subsequently, the contact and roll-off angles of specimens are measured.

Ice adhesion strength measurement: The ice adhesion strengths on SOSs are measured by a digital force gauge (Aipli SF-5, China), indicated in Fig. S13. Prior to measurement, the specimens suffer from 30 s-impact of water jet with $We \sim 34000$, 30 s-impact of ethanol jet with $We \sim 32000$, 30 cycles of Tabler abrasion with 500 g load and ~ 1.5 J of kinetic energy of hammer impact in sequence. And then, the specimen is firstly fixed at the Peltier cooling plate (TEC1-12710), and a cryotube without cap is invertedly placed on the specimen. Then the cryotube is filled with 2 mL water through a man-made hole in its bottom. The water in cryotube is frozen at $-20\text{ }^{\circ}\text{C}$ (with a humidity of $\sim 40\%$) and completely becomes ice cylinder after 1.5 h. Then the force gauge probe is driven to push the cryotube with a speed of 2 mm s^{-1} . The peak forces to detach ice cylinders are recorded. The ice adhesion strengths are calculated by the ratio of the peak force and the cross-sectional area of ice cylinders.

Icing/melting cycle test: The icing/melting cycle tests are carried out in a cooling system which is also used to measure ice adhesion strengths. In this cooling system, two temperature probes with a measurement accuracy of $0.1\text{ }^{\circ}\text{C}$ are installed at the two ends of Peltier cooling plate. A specimen after solid and fluid impact (mentioned above) is firstly fixed in the middle of Peltier cooling plate. During the temperature of Peltier cooling plate falling to $-15\text{ }^{\circ}\text{C}$, several water droplets ($20\text{ }\mu\text{L}$) on the specimen surface gradually freeze. When the $-15\text{ }^{\circ}\text{C}$ is held for 2 min, the cooling system is powered off and the frozen water droplets are rapidly warmed. After 2 min, the frozen water droplets completely melt in the air. In this way, an icing/melting cycle is achieved. Through predetermined icing/melting cycles, the wetting property of n-hexadecane droplets on

the contacting areas is evaluated using surface contact angle analyzer, and meanwhile the ice adhesion strength is also measured by the forementioned method.

$$P_c = \frac{2\gamma_l \cos \theta}{r_p} \quad (1)$$

(γ_l : surface tension of liquid, θ : static contact angle of liquid on solid surface, r_p : effective pore radius of surface texture).

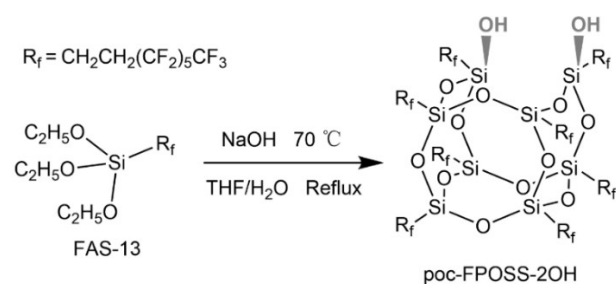


Fig. S1 Synthesis formula of poc-FPOSS-2OH.

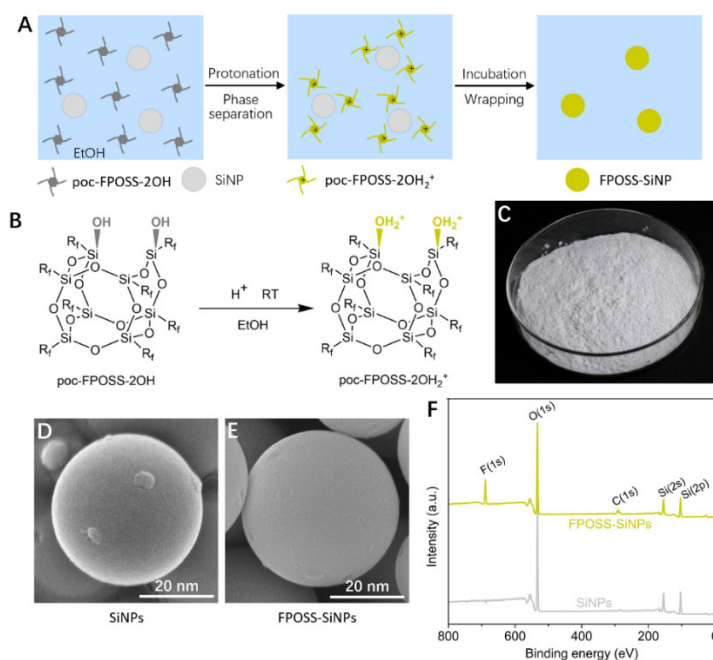


Fig. S2 (A) Schematic illustration of FPOSS-SiNPs. (B) Chemical formulas of poc-FPOSS-2OH₂⁺ formation by acid-triggered protonation of poc-FPOSS-2OH. (C) Photograph of FPOSS-SiNPs. (D) FE-SEM image of SiNPs. (E) FE-SEM image of FPOSS-SiNPs. (F) XPS spectra of SiNPs and FPOSS-SiNPs.

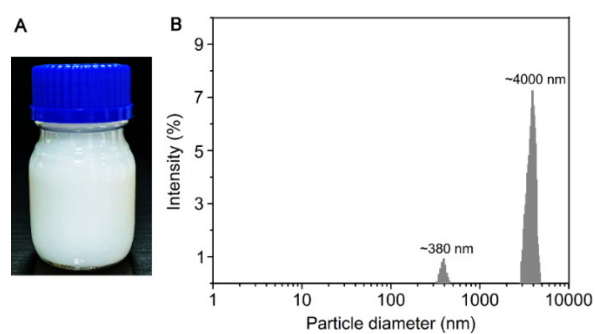


Fig. S3 (A) Photograph of waterborne emulsion. (B) Particle size distribution of waterborne emulsion.

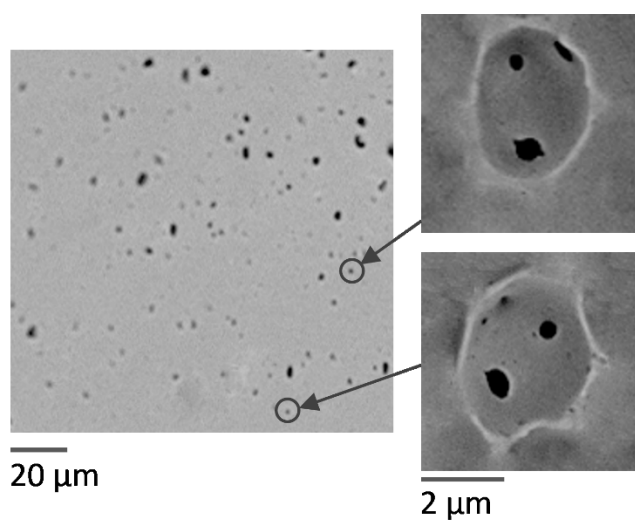


Fig. S4 FE-SEM images of GMI-SOSs from cross-sectional view. Left: low magnification. Right: high magnification of selected area in the left.

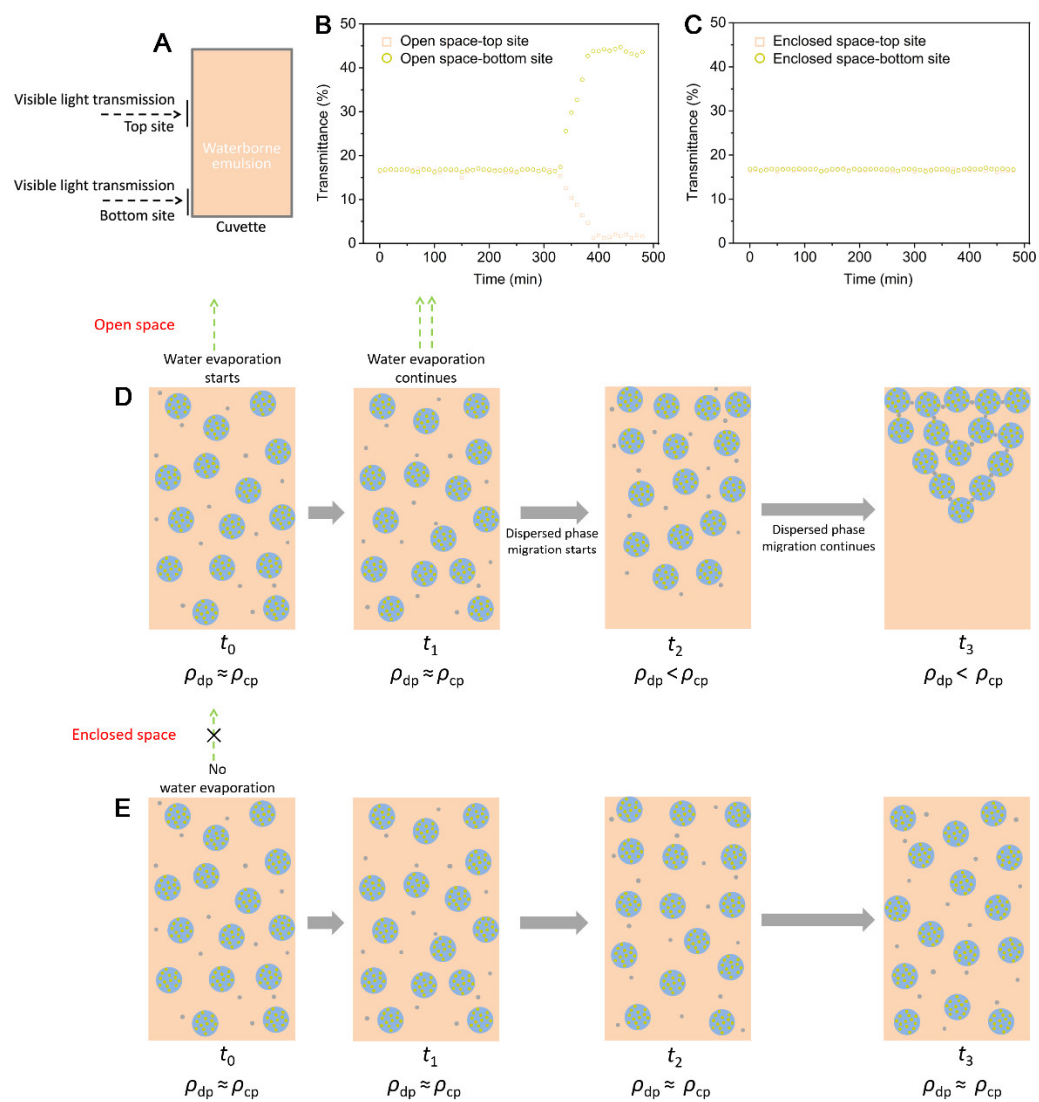


Fig. S5 (A) Schematic illustration of optical transmittance measurement for waterborne emulsion. Plots of transmittance of waterborne emulsion versus standing time in (B) open and (C) enclosed space. Schematic illustration of migration behaviors of dispersed phases in (D) open and (E) enclosed space.

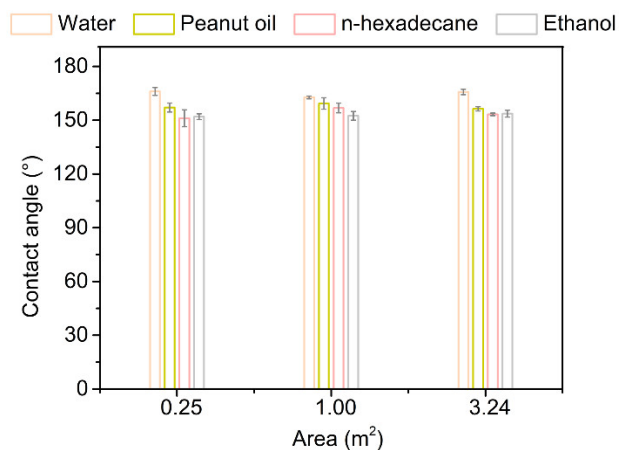


Fig. S6 Plot of contact angle of 4 kinds of liquids on GMI-SOSs versus coating area.

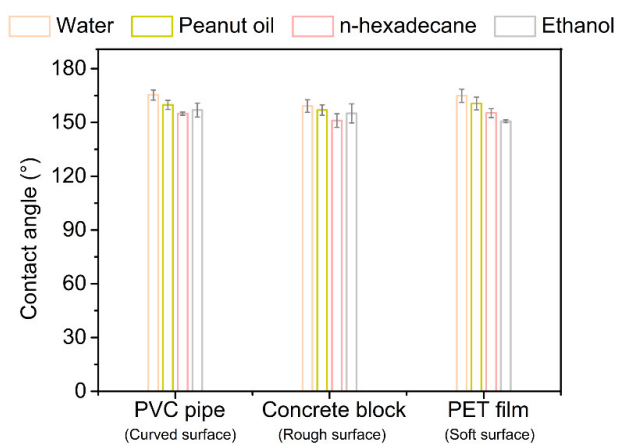


Fig. S7 Plot of contact angle of 4 kinds of liquids on GMI-SOSs formed on PVC pipe (curved surface), concrete block (rough surface) and PET film (soft surface).

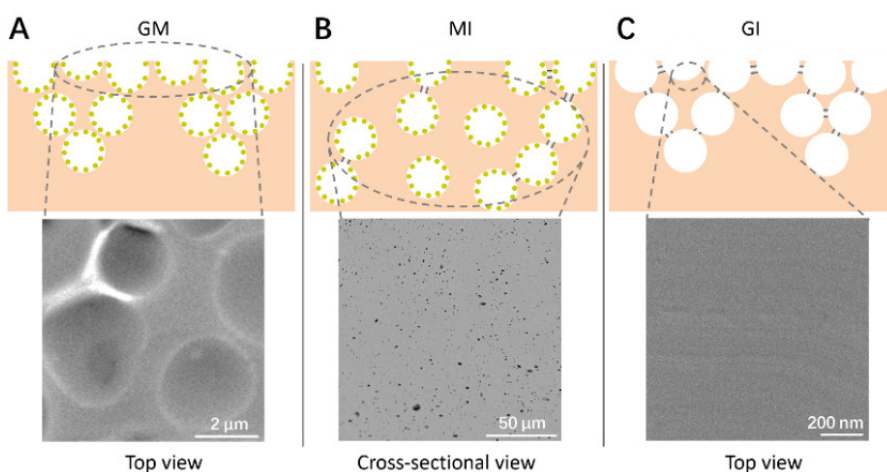


Fig. S8 Schematic illustration and FE-SEM images of SOSs with (A) GM, (B) MI and (C) GI architectures.

$$We = \frac{\rho_l v^2 d}{\gamma_l} \quad (2)$$

(ρ_l : liquid density, v : impact speed of liquid droplet or jet, d : diameter of liquid droplet or jet).

Table S1 Comparison of We of SOS and SHS obtained by bottom-up and top-down strategy.

Order	SHS/SOS	Solvent	Fabrication strategy	Operation method	Drying temperature	Substrate	We	Reference
This work	SOS	Water	Bottom-up	Spray	RT	Not limited	Water: ~48000 Ethanol: ~51000	This work
1	SHS	Water	Bottom-up	Spray	RT	Not limited	Water: ~19800	Ref ³
2	SHS	Organic solvent	Bottom-up	Spray	100 °C	Not limited	Water: ~43000	Ref ⁴
3	SHS	Organic solvent	Bottom-up	Spray	RT	Not limited	Water: 8900	Ref ⁵
4	SHS	Organic solvent	Bottom-up	Spray	RT	Not limited	Water: 3760	Ref ⁶
5	SHS	Organic solvent	Bottom-up	Spray	80 °C	Concrete	Water: 16000	Ref ⁷
6	SOS	Organic solvent	Bottom-up	Spray	70 °C	Not limited	Pentane: 250	Ref ⁸
7	SOS	Organic solvent	Bottom-up	Spray	RT	Not limited	Water: 3641	Ref ⁹
8	SHS	N/A	Top-down	Photolithography + hot/cold-pressing	N/A	Hard substrates	Water: 36478	Ref ¹⁰
9	SOS	N/A	Top-down	Laser machining + hot-pressing	N/A	Metals	Water: >50000	Ref ¹¹
10	SOS	N/A	Top-down	Laser machining	N/A	Hard substrates	Ethanol: >400	Ref ¹²

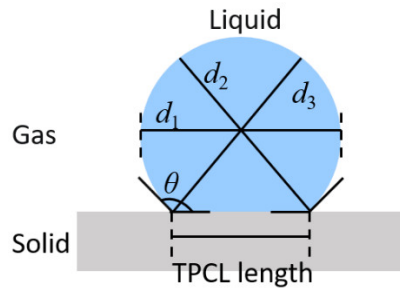


Fig. S9 Schematic illustration of a droplet sitting on a surface, and Laplace pressure P_l is calculated by Equation S3

$$P_l = \frac{2\gamma_l}{r} = \frac{2\gamma_l}{(\sum_1^3 d/2)/3} = \frac{12\gamma_l}{d_1 + d_2 + d_3} \quad (3)$$

(r is the averaged radius of the droplet; d_1 , d_2 and d_3 are illustrated in Fig. S9).

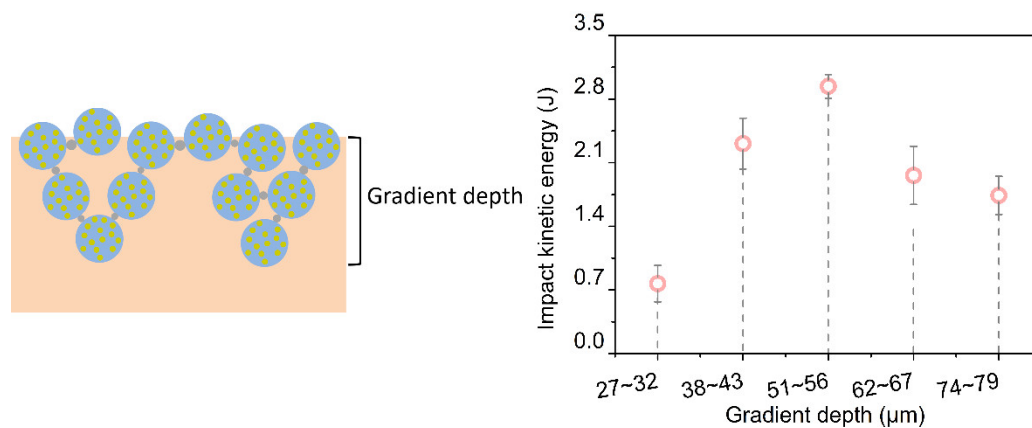


Fig. S10 Left: Schematic illustration of definition of gradient depth. Right: plots of impact kinetic energy (hammer impact) that GMI-SOSs can withstand before losing superomniphobic properties versus gradient depth of GMI-SOSs.

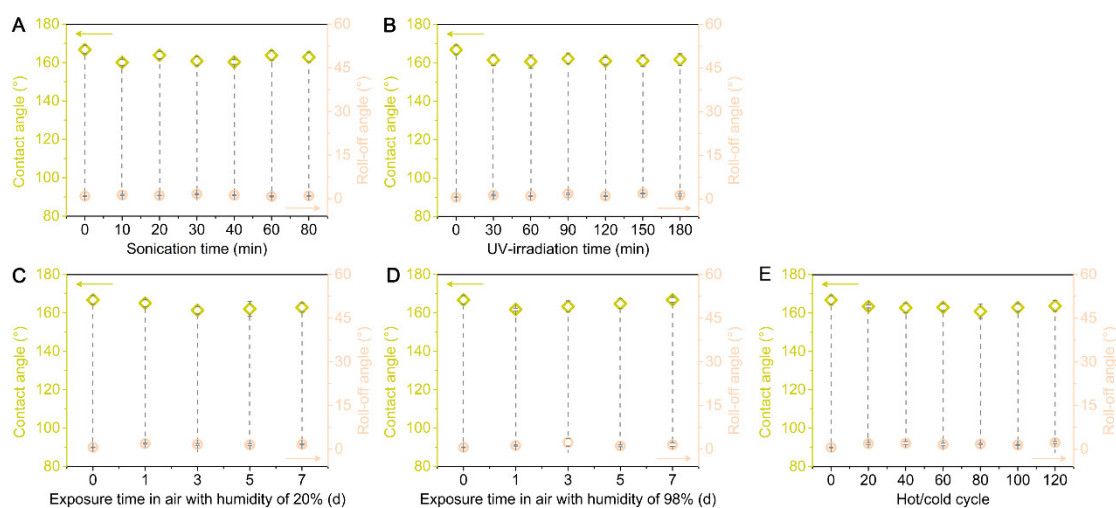


Fig. S11 Plots of contact/roll off angle of water on GMI-SOSs versus (A) sonication time in water, (B) UV-radiation time, (C) exposure time in air with humidity of 20%, (D) exposure time in air with humidity of 80% and (E) hot/cold cycle.

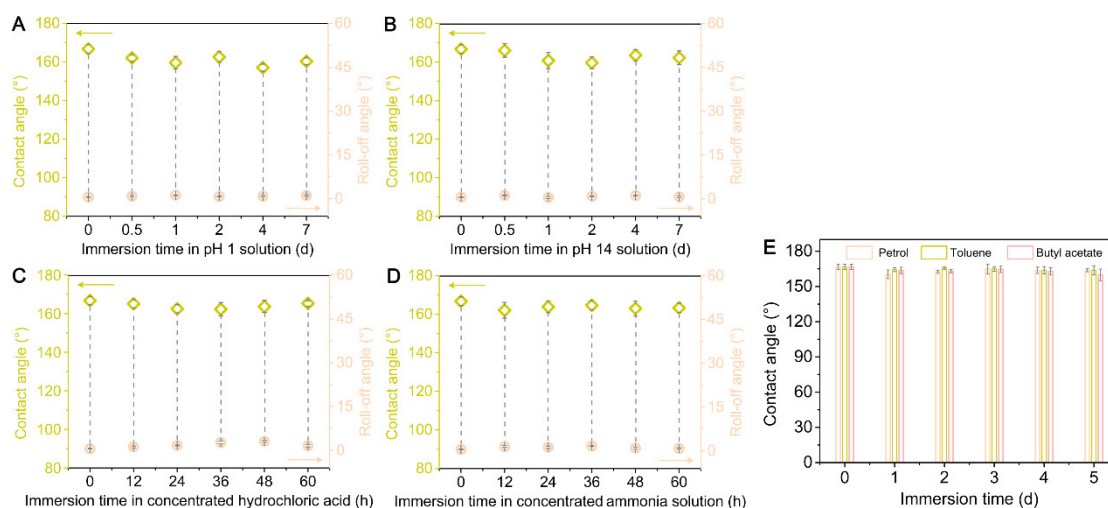


Fig. S12 Plots of contact/roll off angle of water on GMI-SOSs versus immersion time in (A) pH 1 solution, (B) pH 14 solution, (C) concentrated hydrochloric acid, (D) concentrated ammonia solution and (E) organic solvent.

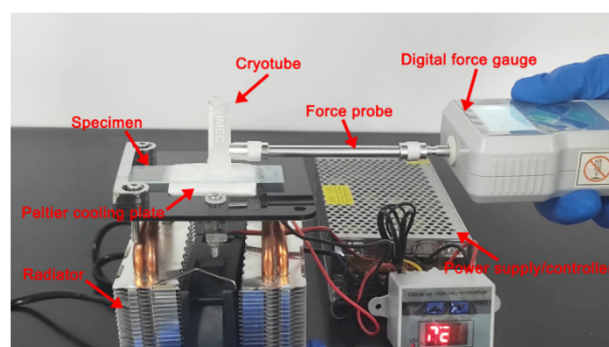


Fig. S13 Photograph of device for ice adhesion strength measurements.

References

- 1 B. Chen, M. Yang, X. Lin, W. Liu, H. Yuan and J. Liao, *Chem. Commun.*, 2022, **58**, 4263-4266.
- 2 B. X. Chen, X. L. Lin, M. J. Yang, Z. L. You, W. F. Liu, H. L. Meng, Y. H. Zhou, H. Yuan and J. W. Liao, *J. Mater. Chem. A*, 2022, **10**, 4944-4951.
- 3 J. Liao, X. Lin, B. Chen, M. Yang, W. Liu, Y. Cao, J. Zhou and J. Zhong, *Nano Lett.*, 2024, **24**, 187-194.
- 4 C. Peng, Z. Chen and M. K. Tiwari, *Nat. Mater.*, 2018, **17**, 355-360.
- 5 H. Luo, M. Yang, D. Li, Q. Wang, W. Zou, J. Xu and N. Zhao, *ACS Appl. Mater. Interfaces*, 2021, **13**, 13813-13821.
- 6 L. Zhang, X. Xue, H. Zhang, Z. Huang and Z. Zhang, *Composites, Part A*, 2021, **146**, 106405.
- 7 Y. Wu, L. Dong, X. Shu, Y. Zhang and Q. Ran, *ACS Appl. Mater. Interfaces*, 2025, **17**, 18852-18868.

8 S. Pan, R. Guo, M. Bjornmalm, J. J. Richardson, L. Li, C. Peng, N. Bertleff-Zieschang, W. Xu, J. Jiang and F. Caruso, *Nat. Mater.*, 2018, **17**, 1040-1047.

9 S. Dong, Y. Li, N. Tian, B. Li, Y. Yang, L. Li and J. Zhang, *ACS Appl. Mater. Interfaces*, 2018, **10**, 41878-41882.

10 D. H. Wang, Q. Q. Sun, M. J. Hokkanen, C. L. Zhang, F. Y. Lin, Q. Liu, S. P. Zhu, T. F. Zhou, Q. Chang, B. He, Q. Zhou, L. Q. Chen, Z. K. Wang, R. H. A. Ras and X. Deng, *Nature*, 2020, **582**, 55-59.

11 D. Li, L. Wang, R. Peng, Z. Song, Z. Liu, Z. Chang, H. Zhang, P. Fan and M. Zhong, *Adv. Sci.*, 2025, **12**, e08272.

12 P. Sun, Y. Jin, Y. Yin, C. Wu, C. Song, Y. Feng, P. Zhou, X. Qin, Y. Niu, Q. Liu, J. Zhang, Z. Wang and X. Hao, *Small Methods*, 2024, **8**, 2201602.